OPEN ACCESS
IOP Publishing | ISECAEP
Journal of Reliability Science and Engineering
J. Reliab. Sci. Eng. **2** (2026) 015401 (20pp)
https://doi.org/10.1088/3050-2454/ae4e8e

A fuzzy cost driven framework for reliability allocation and redundancy analysis: a case study on a multi train evaporation system

Mohammad Rahman*

Engineering, Rio Tinto Group, Charlotte, NC, United States of America

E-mail: m.rahman@unb.ca

Received 7 June 2025, revised 25 February 2026
Accepted for publication 6 March 2026
Published 17 March 2026

Abstract

Industrial process systems often struggle to achieve high availability due to complex interdependencies, limited redundancy, and rapidly escalating costs in high-reliability regimes. This study presents a reliability-centered design review for a wastewater treatment plant's evaporation system, combining reliability block diagram (RBD) modeling with a cost-sensitive reliability allocation framework. Two alternative configurations, series–parallel (equipment-level redundancy) and parallel–series (train-level redundancy) were evaluated. To address the absence of detailed cost data in early design, a dimensionless exponential cost index was developed to represent nonlinear cost escalation as reliability approaches practical limits. This index, derived from fuzzy linguistic ratings and defuzzification, was incorporated into a severity-effort-cost weighting scheme to cascade system-level reliability targets to subsystems and individual equipment. Application to the multi-train evaporation system shows that equipment-level redundancy improves overall system reliability by 11.45% over three months compared with train-level redundancy. The proposed allocation consistently prioritizes failure-prone equipment while avoiding over-investment in already robust units, producing reliability targets that are technically justified and economically rational. The integrated RBD and fuzzy cost-driven allocation framework provides a practical method for early-stage design and retrofit, guiding redundancy planning, focusing improvement actions where they yield the greatest reliability benefits, and enhancing operational resilience in complex engineered systems.

Keywords: series–parallel configuration, *k*-out-of-*n* system, redundancy optimization, reliability allocation, cost-sensitivity

* Author to whom any correspondence should be addressed.

Original content from this work may be used under the terms of the Creative Commons Attribution 4.0 licence. Any further distribution of this work must maintain attribution to the author(s) and the title of the work, journal citation and DOI.

© 2026 The Author(s). Published by IOP Publishing Ltd on behalf of the Institute of Systems Engineering, China Academy of Engineering Physics

1. Introduction

This study addresses the design and reliability optimization of evaporator circuits within a wastewater treatment plant (WWTP) extension, with the objective of maintaining high system availability during the initial nine-month post-commissioning phase, when significantly elevated volume of radioactive wastewater must be treated. To meet this operational requirement, alternative equipment configurations with varying degrees of redundancy are evaluated, and the corresponding individual equipment reliability targets are determined using existing WWTP failure data. Wang [1] outlines four principal strategies for improving system reliability: deploying more reliable components, increasing redundancy, combining these strategies, or modifying the system architecture. This leads to the redundancy allocation problem—optimizing the number, type, and configuration of components to maximize reliability under cost constraints. The selection of appropriate redundancy architecture, including series–parallel, parallel-series, or k-out-of-n configurations depends on specific system requirements and involves trade-offs in reliability, protection against single-point failures and operational flexibility [2]. Ultimately, redundancy levels must balance system criticality, operational risk, and the potential for over-design.

Evaluating system configuration and redundancy options at the design stage is more cost-effective and less disruptive than implementing changes after commissioning, when physical, logistical, and regulatory limitations restrict modification. This work demonstrates the application of reliability block diagram (RBD) modeling to represent the logical dependencies of system equipment in evaporation circuits and quantify their overall system reliability under alternative configurations. Such evaluation enables identification of critical subsystems and demonstrates how configuration choices influence overall system reliability.

While selecting an appropriate configuration is essential for reliable system operation, it alone is not sufficient to ensure that overall system-level reliability targets are met. Achieving these targets requires a deeper evaluation of the functional performance of individual subsystems and equipment, as the system's reliability is ultimately constrained by the most failure-prone equipment. Consequently, design improvements must be implemented at the subsystem or equipment level, where functional failures originate. A structured reliability allocation methodology enables this process by decomposing system-level reliability objectives and cascading them to lower-level equipment using weighted criteria that incorporates historical failure rates, consequence severity, and the technical and economic feasibility of enhancements. This multi-criteria approach ensures that reliability improvements are technically effective, while remaining aligned with practical considerations such as maintainability, state of art technology, and project economics.

The reliability allocation process begins by decomposing a system into subsystems or equipment units and assigning reliability targets using weighted allocation determined based on multiple contributing factors. Over the years, several allocation methodologies have been proposed, each with distinct assumptions and applicability. These include the Aeronautical Radio Inc. (ARINC) method [3], the Advisory Group of Reliability of Electronic Equipment (AGREE) method [4], the Feasibility of Objectives (FOO) method [5], and the Boyd method [6]. More recent approaches include the Critical Flow Method (CFM) [7], the Analytic Critical Flow Method (ACFM) [8], the Integrated Factors Method (IFM) [9, 10], and the Analytic IFM method (A-IFM) [11, 12]. Additional techniques include the Maximum Entropy Ordered Weighted Averaging (ME-OWA) method [13], and FMEA-based approaches that utilize risk priority numbers (RPNs) [14–17]. Chen *et al* [18] modeled failure dependence between subsystems using Copula functions and proposed a relative failure rate-based reliability allocation method, while [19], proposed a goal-oriented reliability allocation approach for multifunction power shift steering transmission to minimize system cost. Despite these contributions, many existing methods overlook the realistic potential for reliability improvement. The FMEA-based approach partially addresses this gap by identifying potential failure modes and recommending corrective actions based on risk ranking [20–22], but their reliance on ordinal scales and single-perspective assessments makes them susceptible to subjective bias. Furthermore, most allocation methods are tailored to systems with simple series configurations, limiting their applicability to more complex architectures. A notable exception is the work of [23], who extended reliability improvement allocation to series–parallel systems with redundant units.

Several cost-based optimization models for reliability allocation have been proposed [24, 25], yet their practical implementation remain limited by the lack of detailed cost information and the need for initial and maximum achievable reliability estimates during early design or retrofit stages [26, 27]. Recent developments have therefore emphasized cost-sensitive and metaheuristic approaches, including harmony search based algorithm using cost-reliability data [28], enhanced zebra optimization with Lévy flight and opposition learning [29], and multifactorial evolutionary algorithms for multi-task optimization [30], alongside comprehensive assessment of redundancy allocation incorporating cost-reliability trade-offs under uncertainty [31]. While these studies underscore the growing trend toward cost-informed, algorithm-driven reliability allocation frameworks, many current methodologies fail to holistically integrate three critical factors: failure severity, which captures the consequence of failure; improvement effort, which reflects the technical difficulty of implementing changes; and economic feasibility, which accounts for the financial constraints associated with reliability enhancement. The absence of a unified framework that incorporates all three dimensions limits the practicality of current methodologies to provide realistic solutions for reliability allocation in complex systems.

To address these limitations, fuzzy and intuitionistic fuzzy approaches have been explored to better represent expert judgment and uncertainties in reliability-redundancy optimization, including signed distance-based defuzzification combined with genetic algorithms [32], intuitionistic fuzzy and chance-constrained approach [33, 34], and Yager's ranking method and multi-level RAP optimization under fuzzy settings [35]. These advances underscore the growing need for integrated fuzzy-based frameworks that can handle imprecision and complexity in reliability allocation. Recognizing these gaps, the present study proposes a unified framework that incorporates expert fuzzy linguistic ratings and defuzzification with cost-sensitive reliability allocation method. Following the selection of an appropriate configuration, system-level reliability targets systematically cascaded to equipment groups and individual equipment through weighted criteria that synthesize failure severity, improvement effort, and cost of enhancement. A key contribution of this study is introduction of a dimensionless cost transformation function, developed from expert insight and practical implementation constraints, to reflect the nonlinear and accelerating nature of cost escalation as systems approach high reliability limits. This improves the practicality of the early-stage reliability allocation, particularly when detailed cost data are limited with the cost acceleration rate calibrated using observed design-cost escalation. Collectively, RBD modeling with this fuzzy, cost-sensitive allocation strategy, the proposed framework provides a structured, data-driven methodology for optimizing reliability-focused design decisions in complex industrial systems.

2. Evaporator system in WWTP

The existing evaporator circuit at the WWTP was originally designed to handle routine wastewater generated during normal facility operations, with a single-train capacity of 75 m^3 d^{-1}. However, the initiation of radioactive waste remediation, particularly the dewatering of deep excavations containing high solids, necessitated a significant capacity upgrade. A new evaporation circuit was therefore designed, comprising three identical trains, each with a capacity of 95 m^3 d^{-1}. Each train includes a feed pump, evaporator vessel, knock-out drum, atmospheric discharge stack, shell-and-tube heat exchanger, and a recirculation pump. Designed to operate in parallel, the system provides operational flexibility and redundancy: one train meets typical demand, while two can be operated concurrently during peak loading, such as the initial nine-month intensive site remediation phase. These trains operate in parallel, providing the plant with redundancy and operational flexibility: one, two, or all three can be operated based on treatment demand.

The existing evaporator system has accumulated considerable operational data that highlights several design limitations. Notably, recurring mechanical seal failures in both the feed and recirculation pumps have led to unplanned downtimes. Additionally, the heat exchangers are prone to scale formation, which reduces heat transfer efficiency and, consequently, evaporation rate. Reduced throughput due to these fouling issues has often necessitated operation of multiple trains, even during periods of moderate demand, increasing energy and maintenance costs. The original system configuration did not incorporate provisions for equipment-level redundancy (standby pumps or bypasses), which has further contributed to reliability concerns. To address these challenges, a reliability focused design assessment was initiated during design phase of WWTP extension project. RBD modeling was employed to represent the logical relationship between subsystem reliability and overall system availability, a well-established method for evaluating impact of component-level reliability and identify areas where redundancy or reliability upgrades yield the highest benefit in complex systems [36].

The RBD analysis for the WWTP extension project was complemented by a structured reliability allocation process, wherein system-level reliability objectives were systematically decomposed and assigned to subsystems using weighted indices based on failure severity, cost of improvement, and implementation effort. This multi-criteria approach enables design upgrades under real-world constraints by prioritizing equipment that exerts the greatest influence on system availability and failure consequences, ensuring that limited upgrade resources are directed toward high-impact areas. The integration of historical failure data with fuzzy logic-based expert judgment for determining allocation weights exemplifies the practical application of reliability engineering in complex process systems.

The reliability of key equipment types within the WWTP, including feed pumps, heat exchangers, and recirculation pumps was estimated using historical failure data from similar units operating under comparable conditions. These records were retrieved from the plant's computerized maintenance management system (CMMS)—SAP. To characterize failure behavior, various statistical life distributions (Weibull, exponential, normal, and lognormal) were evaluated to determine the best fit for observed failure patterns. Among these, the Weibull distribution provided the most accurate representation of mechanical equipment failure characteristics, consistent with prior studies emphasizing its flexibility in modeling diverse failure rate behaviors across mechanical systems [37, 38]. Reliability was then calculated using equation (1), based on the selected Weibull distribution,

$$R(t) = \mathrm{e}^{-\left(\frac{t}{\eta}\right)^{\beta}} \tag{1}$$

where η and β represent the scale and shape parameters, respectively. The estimated Weibull distribution parameters are limited to single failure mode. Therefore, equipment failure data containing competing failure modes (more than one) are separated out and assessed independently for each failure mode.

As shown in the table 1, static equipment, such as the evaporator vessel and heat exchanger, exhibits a wear-out failure pattern and is more reliable during the initial clean-up period. On the other hand, rotating equipment, such as feed pumps and recirculation pumps, shows a predominance of random failures, especially mechanical seal leaks, resulting in significantly lower reliability compared to static components.

Table 1. Weibull parameters from equipment failure data to calculate reliability.

Equipment	Beta, β	Eta, η	Reliability, $\boldsymbol{R_i(t)}$ ($t = 3$ months)
Feed pump	1.04	3.47	42.33%
Evaporator	4.15	78.36	100.00%
Recirculation pump	1.36	6.26	69.29%
Heat exchanger	2.94	37.42	99.94%

3. Optimal system configurations

System or subsystem essential to continuous operation is often designed with redundancy to ensure operational flexibility, accommodate variable production demands, and support both planned and unplanned maintenance activities. In such cases, k-out-of-n configurations are commonly used, maintaining system functionality as long as a minimum number of units remain operational—an approach particularly useful in scenarios when simultaneous operation of all the units is not required. These configurations commonly employ duty-standby arrangements, enabling different combinations of active and standby units based on real-time operation requirements and system conditions. The reliability of k-out-of-n systems can be modeled using the binomial distribution, which describes the probability of functioning the required minimum number of units (k) out of the total (n) under various failure scenarios (figure 1),

$$R_{k-\text{out}-\text{of}-n} = \sum_{i=k}^{n} \binom{n}{k} R^k (1-R)^{n-k}. \tag{2}$$

An RBD was developed for the proposed WWTP extension to evaluate system reliability and identify potential single points of failure. The RBD models the functional interdependencies among components, enabling targeted improvements through redundancies or configuration modification. During the preliminary design phase, two alternative equipment arrangements: a series–parallel configuration and a parallel–series (P–S) configuration were evaluated to understand their influence on the system reliability. The comparative assessment assisted the selection of the optimized system configuration that balances reliability objectives with operational and design constraints.

3.1. P–S configuration

In P–S configuration, as shown in figure 2, each evaporator train consists of individual equipment connected in series, and those trains are connected in parallel to meet system demand. Each evaporator train reliability, R_T is calculated as:

$$R_T = \prod R_{E,\,T} \tag{3}$$

where $R_{E,T}$ represents reliability of individual equipment, $E = \{$feed pump, evaporator, recirculation pump and heat exchanger$\}$ within train, $T = \{A, B \text{ and } C\}$. With P–S configuration, the overall evaporator system reliability during clean-up period, when minimum two trains must remain operational out of three ($k = 2$, $n = 3$), is given by:

$$R_{\text{P}-\text{S}\ (2-\text{out}-\text{of}-3)} = \sum_{k=2}^{3} \binom{3}{2} R_T^k (1-R_T)^{3-k}. \tag{4}$$

Post clean-up activities, only one out of three trains ($k = 1$, $n = 3$) will be required at any given time:

$$R_{\text{P}-\text{S}\ (1-\text{out}-\text{of}-3)} = \sum_{k=1}^{3} \binom{3}{1} R_T^k (1-R_T)^{3-k}. \tag{5}$$

3.2. Series–parallel configuration

The evaporator trains play a crucial role in the WWTP operation. If any equipment fails and requires extended maintenance, the respective evaporator train becomes unavailable due to the lack of operable equipment or low-level redundancy within the trains. To boost system reliability during cleanup period, an interconnection between similar equipment is considered, forming a series–parallel system configuration as illustrated in figure 3. In this configuration, parallel equipment groups are connected in series to provide low-level redundancy. Redundancy at the equipment-level improves the overall system reliability more effectively than train-level redundancy. During clean-up activities, the reliability of an equipment group, R_E where at least two units must be operate out of three ($k = 2$, $n = 3$), is calculated as:

$$R_{E(2-\text{out}-\text{of}-3)} = \sum_{k=2}^{3} \binom{3}{2} R_{E,T}^k (1-R_{E,T})^{3-k}. \tag{6}$$

The equipment group reliability, R_E during post clean-up activities, when only one equipment will be required at any given time ($k = 1$, $n = 3$), can be calculated as:

$$R_{E(1-\text{out}-\text{of}-3)} = \sum_{k=1}^{3} \binom{3}{1} R_{E,T}^k (1-R_{E,T})^{3-k}. \tag{7}$$

Corresponding the overall evaporator system reliability in both cases is given by:

$$R_{\text{S}-\text{P}} = \prod R_E. \tag{8}$$

The series–parallel configuration, characterized by low-level redundancy, is more effective at improving overall system reliability than high-level redundancy. This configuration allows feed-tank flow to be redirected from one evaporator train to another when different equipment failures occur across multiple trains. Table 2 depicts two instances among several possible equipment states during clean-up, where the WWTP must operate of two out of three evaporator trains to meet the demand. When different type of equipment failures arises across multiple trains, the ability to reroute flow becomes essential for sustaining simultaneous operation of two evaporator trains, an operational capability not achievable under P–S configuration.

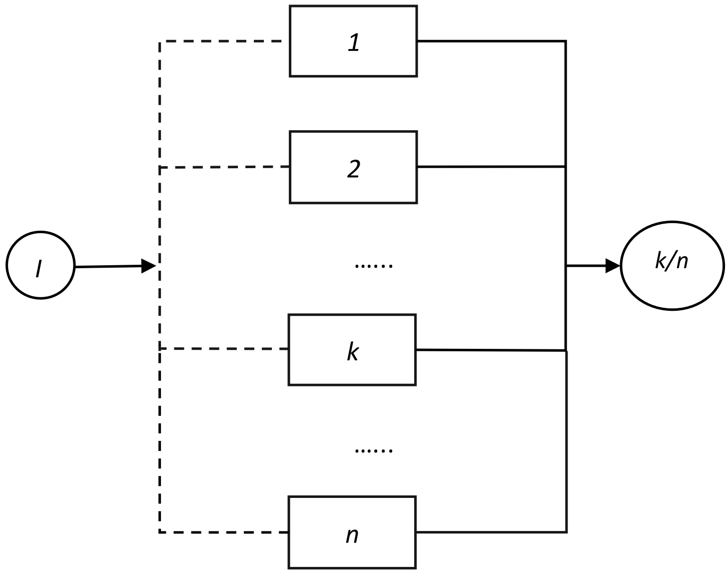

Figure 1. *K*-out-of-*n* system configuration.

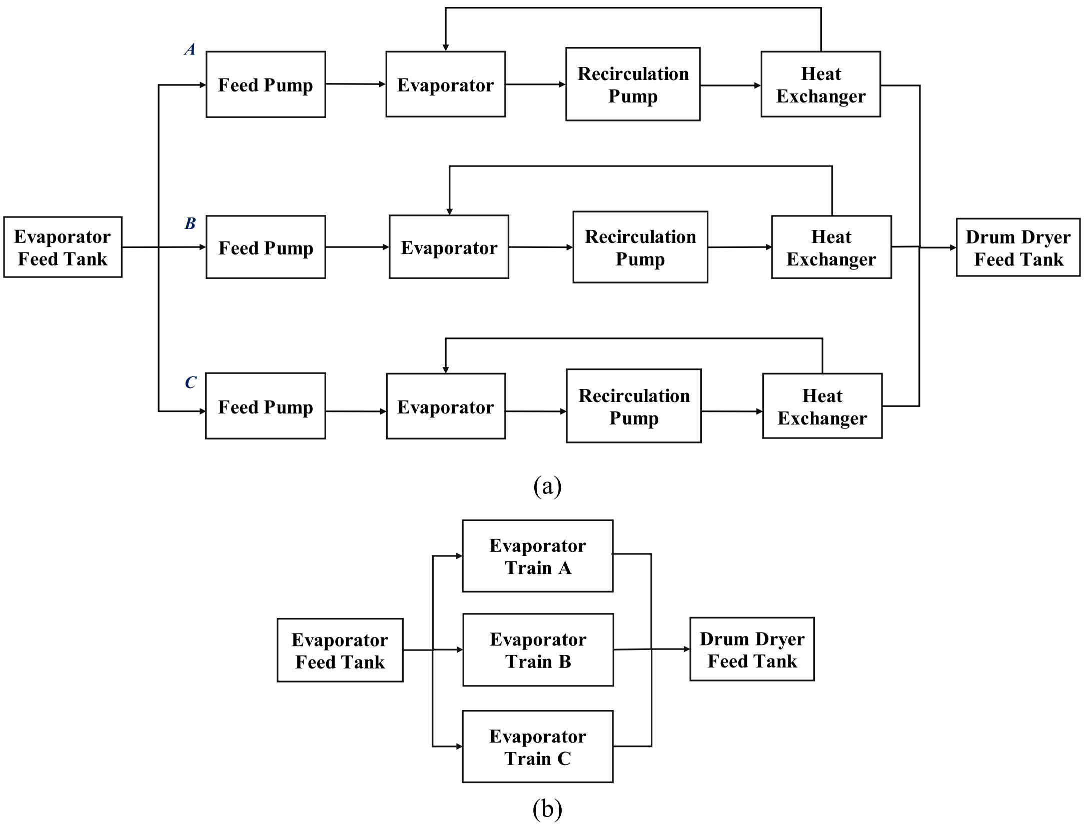

Figure 2. (a) Parallel–series configuration of evaporator system RBD; (b) decomposed and simplified RBD.

Table 3 and figure 4 illustrate the overall system reliability trends for equipment arranged in P–S and series–parallel configurations. During the initial nine-month clean-up period, it becomes evident that the series–parallel configuration, which offers equipment (low) level redundancy, consistently outperforms the P–S configuration. This superiority is reflected in an increase in overall system reliability, reaching a maximum improvement of 11.45% in the third month. These findings underscore the significance of considering equipment or low-level redundancy in industrial systems to achieve optimal reliability. This finding aligns with the Barlow–Proschan (BP) principle [39], which states that, for a coherent system, active redundancy at the component level provides greater reliability than system-level

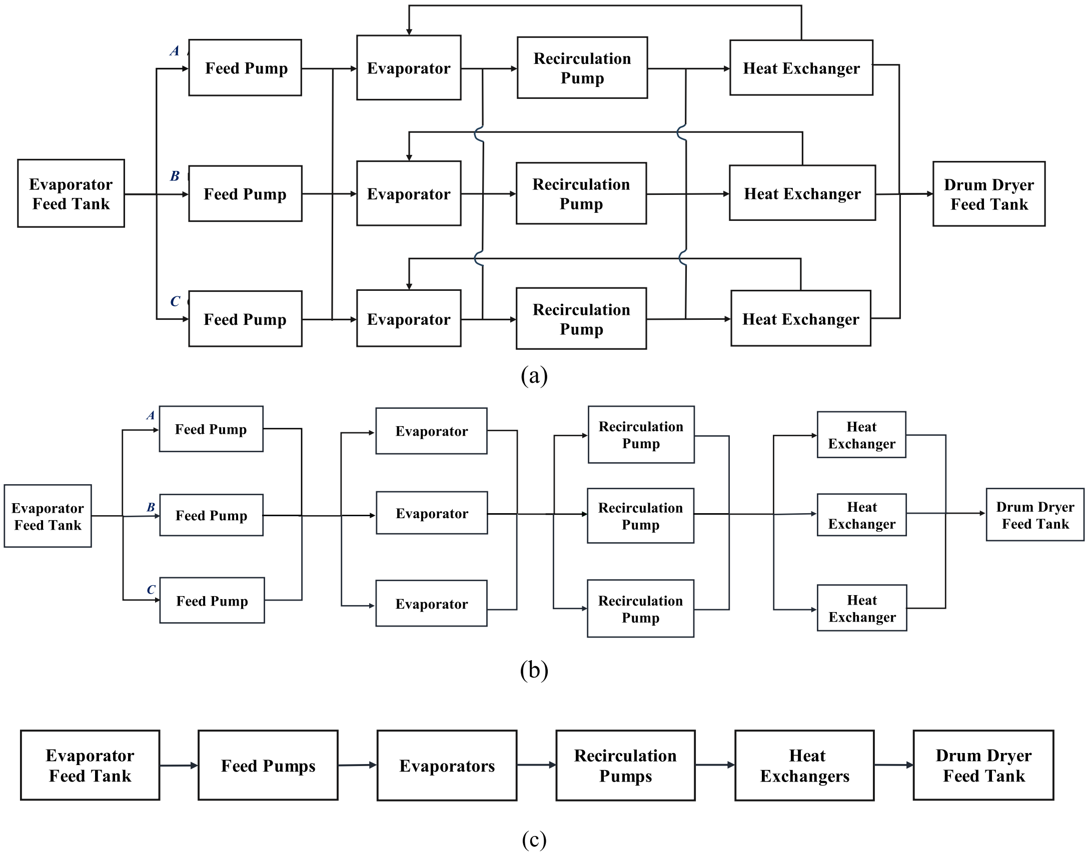

Figure 3. (a) Series–parallel configuration of evaporator RBD; (b) and (c) decomposed and simplified system RBD.

Table 2. Overall system availability scenarios by utilizing sub-system vs equipment level redundancy.

Scenario	Configuration type	Train	Equipment: Feed pump	Equipment: Evaporator	Equipment: Recirculation pump	Equipment: Heat exchanger	Clean-up period system availability (2-out-of-3 train required)
1	Train (high) Level redundancy	A	X	√	√	√	Two train down 50% availability
		B	√	√	√	√	
		C	√	√	X	√	
	Equipment (low) level redundancy	A	X/C	√	√	√	Only one train down 100% availability
		B	√	√	√	√	
		C	√	√	X/A	√	
2	Train (high) level redundancy	A	√	√	√	√	Two train down 50% availability
		B	√	X	√	√	
		C	√	X	X	√	
	Equipment (low) level redundancy	A	√	√	√	√	Only one train down 100% availability
		B	√	X/C	√	√	
		C	√	√	X/B	√	

redundancy under the usual stochastic order for independent components.

The RBD developed in this study represents the specific evaporator system under investigation, capturing its series–parallel configuration and redundancy options. By modifying the component characteristics and interconnections, similar reliability assessment can be performed for the systems commonly found in chemical plants, food processing facilities, power-generation units, and water treatment operations. In practical operation, equipment undergoes periodic maintenance or repairs to prevent functional failures, yet it is reliability cannot be fully restored to an

Table 3. The overall evaporator system reliability calculation with train vs. equipment level redundancy. The higher equipment-level reliability at month 3 is highlighted in bold.

Time (Months)	Parallel–series system/train (high) level redundancy: Train reliability, R_T (equation (3))	Parallel–series system/train (high) level redundancy: System reliability, $R_{\text{P–S (2-out-of-3)}}$ (equation (4))	Series–parallel system/equipment (low) level redundancy: Equipment group reliability, $R_{E\ \text{(2-out-of-3)}}$ (equation (6)): Feed pump	Evaporator	Recirculation pump	Heat exchanger	System reliability, $R_{\text{S–P(2-out-of-3)}}$ (equation (8))
1	70.06%	78.5%	85.6%	100.0%	98.2%	100.0%	84.0%
2	46.08%	44.1%	60.3%	100.0%	90.5%	100.0%	54.6%
3	**29.31%**	**20.7%**	**38.6%**	**100.0%**	**77.5%**	**100.0%**	**29.9%**
4	18.19%	8.7%	23.3%	100.0%	62.1%	100.0%	14.5%
5	11.06%	3.4%	13.6%	100.0%	46.9%	100.0%	6.4%
6	6.60%	1.3%	7.7%	100.0%	33.7%	100.0%	2.6%
7	3.88%	0.4%	4.3%	100.0%	23.2%	100.0%	1.0%
8	2.25%	0.1%	2.4%	100.0%	15.4%	100.0%	0.4%
9	1.29%	0.0%	1.3%	100.0%	9.9%	99.9%	0.1%

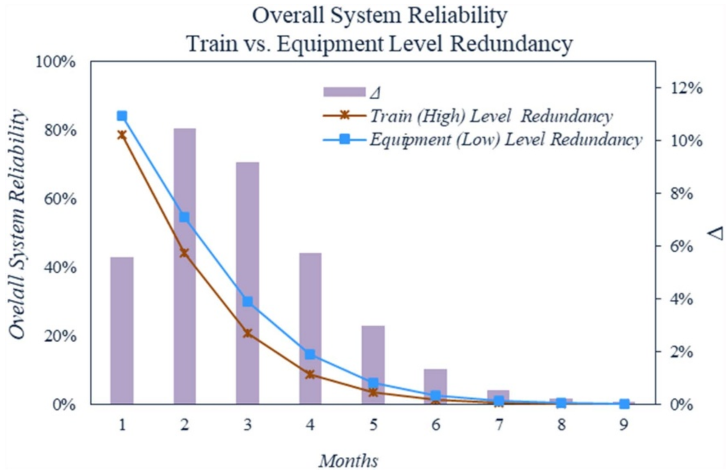

Figure 4. The overall system reliability of the evaporator system for sub-system level vs equipment level redundancy.

'*as-new*' condition. Instead, post-repair reliability typically remains below the original level—a phenomenon known as imperfect repair, as described by (40).

4. Reliability allocation

Once the optimal equipment configuration has been identified, the next step involves establishing the targeted overall reliability for the evaporator system and subsequently allocating this target to the individual equipment level. The reliability allocation process utilizes the FMEA method, which considers the known failure modes of system and sub-system level equipment and provides a realistic allocation that reflects both the targeted improvement and associated implementation challenges. It utilizes the RPN to gauge the impact and frequency of the failure on the system reliability and thereafter, sets reliability allocation targets for corresponding equipment. The RPN for the reliability allocation to the equipment groups or individual equipment under consideration for potential system improvement is given as:

$$\mathrm{RPN}_{ij} = S_{ij} \times O_{ij} \times D_{ij} \tag{9}$$

where, S_{ij} is severity or effect of the failure;

O_{ij} is the occurrence or failure frequency; and

D_{ij} is detectability of the failure with current control system

In many practical settings, detectability is assumed to be inherently captured in severity, especially in systems with consistent diagnostic capabilities. The detection ranking is not included in the RPN calculation because the detection of a failure mode is considered when assigning a severity ranking. Yadav *et al* [41], and Itabashi-Campbell and Yadav [42] proposed the average RPN as a measure of failure criticality for systems with N failure modes, defined as follows:

$$K_i = \frac{1}{N}\sum_{j=1}^{N}\left(S_{ij} \times O_{ij}\right) \quad . \tag{10}$$

The criticality index enhances the prioritization framework by providing a more nuanced indication of the urgency for reliability improvements. This prioritization process benefits significantly from the incorporation of expert knowledge, wherein maintenance and reliability professionals contribute their domain-specific insights to enable a more comprehensive and context-sensitive assessment of system vulnerabilities. However, despite its utility, several limitations are inherent in traditional risk prioritization methods, particularly the use of the RPN. Xiao *et al* [43], highlighted that assigning equal weighting to severity, occurrence, and detectability in the RPN calculation can generate misleading equivalencies, where failure modes with identical RPN values may arise from different combinations of risk factors and yet differ markedly in their real-world consequence. Furthermore, conventional RPN-based models typically do not incorporate the technical difficulty or economic cost associated with improving the subsystem reliability from its current baseline, limiting their applicability in developing practical and cost-effective improvement strategies.

Fuzzy-based reliability allocation methods have gained increasing attention due to their ability to integrate subjective expert judgment with structured decision-making frameworks. For instance, [44], incorporated product development risk when selecting influencing factors and determining weights through a fuzzy analytic hierarchy process (FAHP), enabling graded assessment of component reliability in early-stage design; [45], applied trapezoidal fuzzy division linear programming to synthesize diverse expert opinions during the evaluation of reliability allocation factors for a transceiver system in the early-stage design; [46], employed intuitionistic trapezoidal fuzzy numbers and a performance ranking method based on ideal solutions to perform reliability allocation for CNC machine tools; and [47], introduced factor equivalence evaluation sets and expert authority coefficients to reflect heterogeneous factor influence and expert familiarity, resulting in more robust and realistic allocation outcomes. Building on this foundation, the current study adopts a fuzzy linguistic rating and defuzzification to evaluate both failure mode criticality and cost-related attributes associated with reliability improvement. This addresses a key limitation in traditional approaches—the use of ordinal severity scales, which assign

Table 4. Linguistic terms used to evaluate the weights of the criteria.

Linguistic terms	Triangular fuzzy number
Very low (VL)	(1, 1, 3)
Low (L)	(1, 3, 5)
Medium (M)	(3, 5, 7)
High (H)	(5, 7, 9)
Very high (VH)	(7, 9, 9)

a single integer value to represent complex failure outcomes. Such scales often fail to capture the intricacy of real-world engineering judgments and may introduce bias or oversimplification. In contrast, the fuzzy linguistic process allows experts to express their assessments through qualitative linguistic terms (e.g. low, medium, high), which are more intuitive and better aligned with practical engineering experience.

Three experienced maintenance and operations professionals with extensive domain knowledge of the WWTP participated in the fuzzy-based evaluation. Their linguistic ratings were systematically transformed into quantitative scores using fuzzy aggregation and defuzzification techniques, ensuring a rigorous yet realistic decision-making process. The linguistic scales and their corresponding triangular fuzzy number (TFN) mappings are presented in table 4, with a visual depiction shown in figure 5.

The fuzzy linguistic terms assigned to each criterion by q experts are aggregated using the arithmetic mean into a fuzzy rating, denoted as:

$$\tilde{a} = \left(\tilde{l}, \tilde{m}, \tilde{u}\right) \tag{11}$$

$$\tilde{l} = \frac{1}{q}\sum_{q=1}^{q}\{l_k\} \tag{12}$$

$$\tilde{m} = \frac{1}{q}\sum_{q=1}^{q}\{m_k\} \tag{13}$$

$$\tilde{u} = \frac{1}{q}\sum_{q=1}^{q}\{u_k\} \tag{14}$$

where l, m and u represent the lower bound, most likely value and upper bound of the aggregated TFN, respectively.

The aggregated fuzzy ratings are then defuzzified into crisp numerical values using centroid method:

$$a = \frac{\tilde{l} + \tilde{m} + \tilde{u}}{3}. \tag{15}$$

This approach ensures that the reliability prioritization process remains both rigorous and flexible, bridging the gap between theoretical modeling and practical engineering insight. The linguistic scales in table 4 map to TFNs that are nearly symmetric around their most likely value. When defuzzification is performed via the centroid method, symmetric TFNs yield a crisp value identical to the modal term, irrespective of the TFN spread. This mathematical property ensures that defuzzified values remain invariant under symmetric conditions. Table 5 presents the failure rates and corresponding linguistic severity ratings assigned by three operations and maintenance experts for each failure mode associated with WWTP equipment.

4.1. Severity index

Design improvements should prioritize equipment associated with high-severity failure modes. Subsystem with higher severity ratings must be prioritized and receive greater investment during design improvement. Kim *et al* [14], highlighted a critical limitation of the conventional ordinal scale, which assumes a linear relationship between the assigned severity score and the actual impact of failure. In practice, failure consequences often increase nonlinearly with severity. To address this, they proposed a transformed severity rating based on a monotonic increasing function of the most critical failure mode within a subsystem. This transformation more accurately reflects the disproportionate impact of high-severity failures, ensuring that components with the most critical consequences receive appropriately increased weight in reliability allocation process.

The severity of failure for a given equipment unit i across multiple criteria j is defined as:

$$S_{ij} = \max\left(S_{i1}, S_{i2}, .., S_{ij}\right). \tag{16}$$

To enhance the distinction among severity ratings, an exponential transformation is applied:

$$\bar{S}_{ij} = \exp\left(\alpha S_{ij}\right) \tag{17}$$

where α is the designer-selected severity amplification coefficient that reflects the desired emphasis placed on high-severity failure modes. A higher α increases the weight assigned to subsystems with severe failure consequences, thereby elevating their priority in reliability improvement strategies.

The normalized severity rating is then expressed as:

$$s_i = \frac{\bar{S}_i}{\sum_{i=1}^{N}\bar{S}_i}. \tag{18}$$

4.2. Improvement effort

Like severity, subsystem with higher failure rates exhibit higher potential for improvement with comparatively less effort. Yadav and Zhuang [48], proposed a mathematical model illustrating a monotone-decreasing relationship between failure rate and the effort required for reliability improvement. They argue that highly reliable subsystem requires substantially more effort to achieve additional reliability gains, where as subsystem with higher failure rates (i.e. lower inherent reliability) require less effort for the same incremental improvement. Consequently, subsystem with higher failure rates should be assigned higher weight in reliability allocation decision.

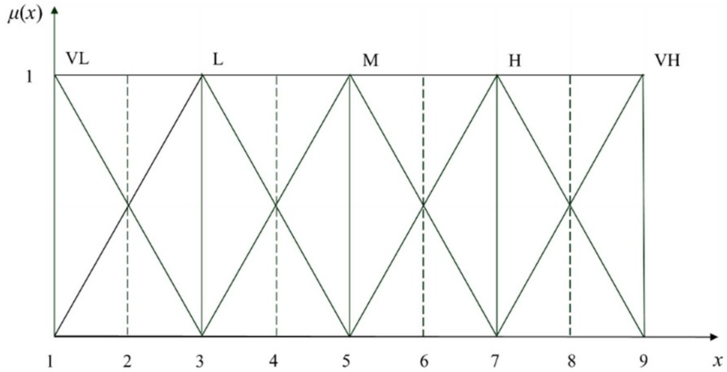

Figure 5. Linguistic scale for evaluating criteria weight in reliability allocation.

Table 5. Fuzzy severity assessment and failure rates for failure modes associated with each equipment in the evaporator circuit.

				Fuzzy ratings						
i	Equipment	j	Failure modes	E1	E2	E3	Aggregated severity	Crisp severity S_{ij} (equation (15))	λ_{ij}	λ_i
1	Feed pumps	1	Seal leaking	VH	H	VH	(6.33, 8.33, 9)	7.89	0.090 280	0.293 084
		2	Bearing failure due to lack of lubrication	VH	VH	H	(6.33, 8.33, 9)	7.89	0.061 444	
		3	High vibration	H	H	H	(5, 7, 9)	7	0.040 500	
		4	Misalignment	H	M	H	(5.67, 7, 9)	7.22	0.023 190	
		5	Impeller/suction line clogged	H	H	H	(5, 7, 9)	7	0.021 799	
		6	Excess power draw	H	M	M	(5, 5.67, 7.67)	6.11	0.021 180	
		7	Shaft deflection	M	H	H	(5.67, 7, 9)	7.22	0.020 381	
		8	Dry running	M	H	H	(5.67, 7, 9)	7.22	0.010 300	
		9	Power monitor failure	L	VL	L	(1.89, 2.33, 3.67)	2.63	0.004 011	
2	Evaporator	1	Nozzles leak due to corrosion	H	H	H	(5, 7, 9)	7	0.007 452	0.014049
		2	Corrosion under insulation	H	H	M	(5.67, 7, 9)	7.22	0.003 142	
		3	Support weld crack	M	M	H	(5, 5.67, 7.67)	6.11	0.002 018	
		4	Insulation degradation	L	L	L	(1, 3, 5)	3	0.001 438	
3	Recirculation Pump	1	Seal leaking	VH	H	VH	(6.33, 8.33, 9)	7.89	0.100 420	0.174 373
		2	High vibration	H	H	H	(5, 7, 9)	7	0.042 101	
		3	Bearing failure due to lack of greasing	VH	VH	H	(6.33, 8.33, 9)	7.89	0.029 503	
		4	Cavitation	M	M	L	(4.33, 5, 6.33)	5.22	0.002 353	
4	Heat Exchanger	1	Gasket cracking and swelling	H	M	M	(5.67, 7, 9)	7.22	0.016 106	0.025 415
		2	Plate fouling	M	M	L	(4.33, 5, 6.33)	5.22	0.010 407	
		3	Internal clogging	L	M	L	(3, 4.33, 5.67)	4.33	0.003 442	

The improvement effort, expressed as a function of failure rate, is given by:

$$E_i = -\frac{ln\lambda_i}{r} \tag{19}$$

where λ_i represents the failure rate of subsystem i, and r is a decreasing improvement rate that captures the sensitivity of required effort to changes in failure rate. This expression aligns with the practical reliability engineering insight: subsystems with higher failure rates typically provide more potential for effective improvement, while system that are already highly reliable yield diminishing returns.

To support comparative analysis across subsystems, the improvement effort is normalized as:

$$e_i = \frac{E_i}{\sum_{i=1}^{N} E_i}. \tag{20}$$

4.3. Proposed cost index

While effort reflects the technical feasibility of implementing reliability improvements, cost captures the associated economic burden, which often limits or constrains such enhancements. In practical cases, especially during conceptual design or early-phase retrofit planning, precise cost data for reliability improvement is either unavailable or infeasible to collect. As noted by [26], and [27], although reliability–cost relationships can ideally be constructed from historical data, such data sets are often sparse or inaccessible. To address this challenge, [27], proposed a nonlinear cost function to quantify the cost of improving subsystem reliability:

$$C_i\left(R_i\right) = \exp^{\left[(1-f_i)\frac{R_i - R_{i,\,\min}}{R_{i,\,\max} - R_i}\right]} \tag{21}$$

where R_i denotes allocated reliability target for subsystem *i*, $f_i \in (0, 1)$ is a coefficient reflecting the feasibility of reliability enhancement, $R_{i,\,\min}$ and $R_{i,\,\max}$ represent the current and maximum achievable reliability levels, respectively; and $C_i\left(R_i\right)$ indicates the costs associated with improving reliability from $R_{i,\,\min}$ to R_i.

A range of additional cost models have emerged in the literature. Recently, [49], proposed a logarithmic cost function that incorporates influencing factors such as subsystem complexity, operating environment, and technological maturity as proxies for economic burden, highlighting that the subsystem reliability improvement cost is constrained by the initial and maximum achievable reliability levels under given design and operational conditions. Elegbede *et al* [24], likewise outlined critical conditions that any valid cost function must satisfy, consistent with earlier work by [25, 50, 51] and who emphasized the disproportionate escalation of cost as system reliability approaches its theoretical upper limit.

Recognizing the limitations of quantitative cost modeling, especially when the detailed financial data are unavailable, this study introduces a dimensionless cost index, C_i to represent the economic difficulty of improving individual subsystems. Rather than quantifying monetary cost directly, the index incorporates qualitative attributes known to correlate with the expense of reliability improvements. Such attributes have been widely used in the literature to construct allocation weights [5, 8, 52]. The present study extends this practice by employing similar attributes as qualitative surrogates for cost–escalation trends when detailed monetary data are unavailable. A fuzzy linguistic assessment was used to capture expert judgment: each subsystem was rated using predefined linguistic terms across four key cost dimensions (e.g. low, medium, high). The aspects of these attributes and the considerations used to rank them within the WWTP system are detailed below:

- A_{i1}: System intricacy—this factor reflects the structural and functional complexity of the subsystem, including component count, interface intricacy, and cross-domain interactions (e.g. mechanical-electrical, hydraulic system). A higher intricacy generally implies greater design constraints, higher integration risk, and increased cost for reliability improvement. In this study, both feed and recirculation pumps exhibit high intricacy due to the presence of multiple rotating components, bearings, seals, couplings, monitoring and control instrumentation. The integration of these elements significantly elevates their improvement effort and cost, lefting their very high rating. In contrast, evaporator, and heat exchanger are simple static equipment with minimal instrumentations and are therefore rated medium.
- A_{i2}: State of Art design—this dimension reflects subsystem's potential for modernization, modular upgrades, and design flexibility. Low scores generally indicate mature or legacy architectures with limited scope for innovation. The pumps offer significant upgrade potential, including corrosion-resistant liners, improved API seal plans, and component standardization, and are thus rated very high. Conversely, the evaporator and heat exchanger rely on well-established standardized designs with limited scope for improvement are therefore rated low.
- A_{i3}: Maintainability—this dimension reflects the design cost required to enhance maintainability, including improved service access, modular disassembly features, and the integration of condition-monitoring and fault-isolation mechanisms. In this study, the pumps exhibit poor maintainability due to complex disassembly procedures and non-modular construction, contributing to extended downtimes and elevated redesign costs; they are consequently rated high. In contrast, the evaporator and heat exchanger contain fewer moving parts and follow simpler maintenance protocols, requiring lower redesign effort and are thus rated medium to low.
- A_{i4}: Environmental—this factor evaluates the impact of adverse operating conditions characterized by elevated temperature, humidity, corrosive or abrasive media, and cyclic loading. Equipment exposed to harsh conditions typically demands more robust materials or protective systems, increasing both the cost and complexity of reliability improvements. In the current WWTP application, all subsystems encounter moderate process environments involving biological fouling, scaling, and variable flow conditions, resulting in a medium rating applied across all subsystems.

These attributes interact rather than contribute independently. The four dimensions function as orthogonal, cost–increasing factors, and their multiplicative combination captures the escalating cost associated with simultaneously high ratings. The product form preserves their compounding influence and avoids additive compensation, ensuring that a subsystem scoring low on one dimension is not offset by high ratings on others.

Given these considerations, the composite cost index, C_i for each equipment is computed as:

$$C_i = A_{i1} \cdot A_{i2} \cdot A_{i3} \cdot A_{i4}. \tag{22}$$

This formulation serves as qualitative proxies for cost escalation, with each factor contributes positively to the difficulty

Table 6. Fuzzy expert rating for evaluating equipment cost indices.

		A_{i1}			A_{i2}			A_{i3}			A_{i4}		
i	Equipment	E1	E2	E3	E1	E2	E3	E1	E2	E3	E1	E2	E3
1	Feed pumps	H	VH	H	H	H	H	VH	VH	H	M	M	M
2	Evaporator	M	L	L	L	M	L	M	H	M	L	M	M
3	Recirculation pump	H	H	M	VH	H	H	H	VH	H	M	M	M
4	Heat exchanger	M	M	L	M	L	L	L	M	L	M	L	M

and cost of improving subsystem reliability. These ratings were then converted to triangular fuzzy numbers to accommodate uncertainty and subjective variability among experts. Aggregation and defuzzification techniques were applied to synthesize these into a single crisp numerical value for each factor. By integrating linguistic ratings into a structured fuzzy logic framework, the proposed cost index maintains analytical rigor while allowing flexibility to accommodate expert judgment. This enhances the practical utility of the model for design evaluation, prioritization of reliability investments, and trade-off studies under conditions of limited data.

Table 6 presents the fuzzy linguistic ratings provided by three operations and maintenance experts for four cost factors influencing reliability improvement. Table 7 summarizes the aggregated fuzzy ratings and the calculated composite cost index for each equipment.

While C_i provides a useful composite measure, it does not fully capture the inherently non-linear and rapidly increasing costs associated with an incremental reliability enhancement. To better model this escalation behavior, the raw cost index, C_i is transformed into a dimensionless, exponentially scaled index, $\bar{C}_i$ using:

$$\bar{C}_i = \exp\left(\theta \cdot \frac{C_i}{C_{\max} - C_i}\right) \tag{23}$$

where $C_{\max}$ is the theoretical upper limit of the cost index (taken as $C_{\max} = 9^4 = 6561$ in present study), θ is a positive growth-rate parameter governing how sharply costs escalate as the design approaches its feasible complexity limit. The transformed cost index, $\bar{C}_i$ is subsequently used within optimization framework. This exponential transformation ensures three critical properties essential for modeling cost escalation behavior in reliability-driven design:

(i) Positivity: $\bar{C}_i > 0$ for all $0 < C_i < C_{\max}$;
(ii) Monotonicity: $\bar{C}_i$ is always increasing with C_i; and
(iii) Rapid Growth: As $C_i \to C_{\max}$, $\overline{C_i} \to \infty$, reflecting the steep cost escalation typically required near maximum design limit.

The transformed cost index, $\bar{C}_i$ serves as a dimensionless indicator of the relative escalation of reliability improvement costs, capturing the characteristic reliability–cost trade–off, rather than absolute monetary values. This transformation enables consistent comparison across equipment and supports cost-weighted allocation in multi-component systems. The exponential transformation ensures that $\bar{C}_i \to 1$ as $C_i \to 0$, establishing a normalized lower bound that that represents the minimal cost associated with limited opportunities for reliability improvement. This limiting behavior is consistent with empirical cost-growth trends noted by [27], and the functional properties outlined by [24]. The cost escalation parameter, θ governs the rate at which $\bar{C}_i$ increase as C_i approaches the design maximum, reflecting the nonlinear nature of cost amplification in high-reliability regimes.

To estimate a physically meaningful value of θ, an escalation constraint representative of observed mid-range design behavior: a 20% increase in the mid-range defuzzified cost index, C_i doubles the transformed cost, $\bar{C}_i$:

$$\bar{C}_i\,(1.2C_i;\theta) = 2 \cdot \bar{C}_i\,(C_i;\theta). \tag{24}$$

This condition ensures that the accelerated growth behavior is embedded in $\bar{C}_i$, capturing the nonlinear cost amplification characteristic as designs approach saturation limits. It reflects a case-specific observation that incremental design enhancements, particularly near mid-range complexity, tend to escalate costs disproportionately relative to the resulting reliability gains. In industrial systems, even modest expansions in design scope can trigger substantial increase in expenditure due to compounding factors such as specialized component integration, increased manufacturing complexity, tighter tolerances and more stringent quality-assurance requirements. Within the evaporation trains, for example, upgrades to slurry pumps, including double mechanical seals, seal–flush instrumentation, and distributed control system (DCS) integration etc, significantly elevate material, installation, and commissioning costs. In addition, deployment of remote condition–monitoring infrastructure adds further expense through sensors, communication hardware, cybersecurity validation, and ongoing data–management requirements. On the static equipment side, specifying corrosion-resistant evaporator and heat exchanger vessels (e.g. higher-grade steel or advanced alloys) amplifies material and fabrication costs, and often requires more stringent welding and QA/QC procedures. Collectively, these factors yield nonlinear cost escalation, often several-fold above the baseline designs.

Although not universally fixed, this escalation condition is selected based on historical project behavior and expert judgment, serving as a designer-defined benchmark for capturing the rapid cost amplification typical of high-reliability targets. By substituting equation (23) for both values:

$$\exp\left(\theta \cdot \frac{1.2C_i}{C_{\max} - 1.2C_i}\right) = 2 \cdot \exp\left(\theta \cdot \frac{C_i}{C_{\max} - C_i}\right). \tag{25}$$

Table 7. Aggregated fuzzy ratings, defuzzified values, and composite cost index (C_i) for equipment.

i	Equipment	Aggregated fuzzy ratings				Crisp fuzzy numbers (equation (15))				C_i (equation (22))
		A_{i1}	A_{i2}	A_{i3}	A_{i4}	A_{i1}	A_{i2}	A_{i3}	A_{i4}	
1	Feed pumps	(6.33, 8.33, 9.00)	(5.00, 7.00, 9.00)	(6.33, 8.33, 9.00)	(3.00, 5.00, 7.00)	7.89	7.00	7.89	5.00	2178.82
2	Evaporator	(2.33, 3.00, 4.33)	(1.67, 3.67, 5.00)	(4.00, 6.00, 7.00)	(2.33, 4.33, 5.67)	3.22	3.44	5.67	4.11	258.13
3	Recirculation pump	(5.67, 7.00, 8.33)	(6.33, 8.33, 9.00)	(6.33, 8.33, 9.00)	(3.00, 5.00, 7.00)	7.00	7.89	7.89	5.00	2178.82
4	Heat exchanger	(3.00, 4.33, 5.67)	(2.33, 3.00, 4.33)	(2.00, 3.67, 5.67)	(3.00, 4.33, 5.67)	4.33	3.22	3.78	4.33	228.20

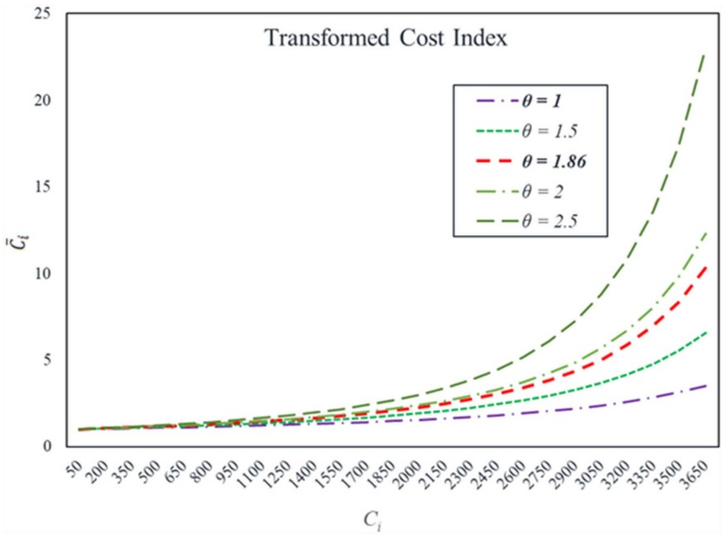

Figure 6. Transformed cost index, $\bar{C}_i$ versus C_i. Larger θ produces steeper escalation as the design approaches its maximum feasible complexity.

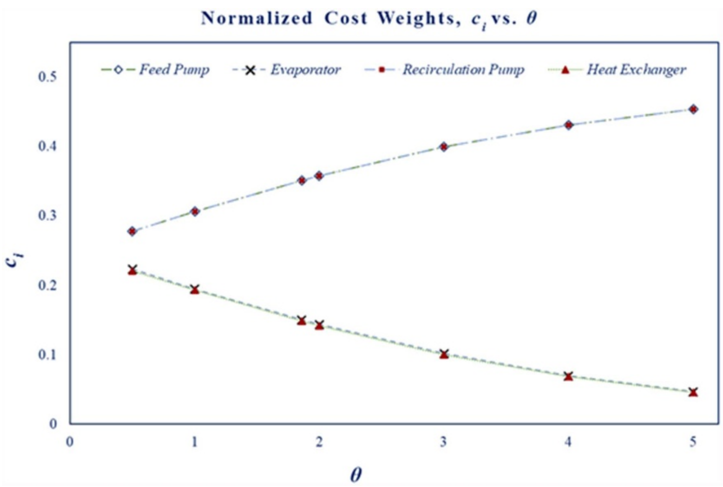

Figure 7. Normalized cost index, $c_i(\theta)$ versus escalation parameter, θ. Increasing θ concentrates the cost burden in the pumps and reduces it for the evaporator and heat exchanger.

Choosing a mid-range complexity base cost index, $C_i = 3000$, $C_{\max} = 9^4 = 6561$ and taking natural logarithm of both sides yields:

$$\theta \cdot \frac{3600}{2961} = \ln(2) + \theta \cdot \frac{3000}{3561}. \tag{26}$$

Solving equation (26) algebraically provides $\theta \approx 1.86$. The corresponding exponential cost curve, shown in figure 6, illustrates how the transformed cost index rises sharply as C_i approaches $C_{\max}$. The figure also illustrates the impact of different θ, highlighting how choice of escalation parameter influences cost-growth behavior.

For integration into a normalized reliability allocation framework, the transformed cost index is further scaled as:

$$c_i = \frac{\bar{C}_i}{\sum_{i=1}^{N} \bar{C}_i}. \tag{27}$$

4.4. Influence of θ on normalized cost allocation

Using the defuzzified composite indices, C_i from table 7 and $C_{\max} = 9^4$, the transformed cost index, $\bar{C}_i$ and normalized cost weights, c_i were evaluated across θ as shown in figure 7. The rank ordering of subsystem remains invariant (pumps > evaporator $\gtrsim$ heat exchanger) but increasing θ amplifies cost discrimination: the cost weight of feed and recirculation pumps rise with θ, whereas those of evaporator and heat-exchanger decline. In contrast, direct normalization of raw composite index, C_i (without exponential transformation with growth-rate parameter, θ) yields a constant c_i values, confirming that the observed shifts arise solely from exponential mapping controlled by θ.

As illustrated in figure 7, increasing θ amplifies the relative penalty applied to equipment with higher defuzzified cost indices, C_i. Between $\theta = 1$ and $\theta = 5$, the normalized cost share for each pump increases from ~0.31 to 0.45, while the evaporator and heat exchanger decline sharply from ~0.19

to 0.05. These trends reflect the nonlinear escalation characteristic of the exponential cost transform and illustrate how stronger cost escalation conditions concentrate the total cost burden in rotating equipment, while reducing it for static equipment. Because the pumps exhibit substantially larger C_i values than the static equipment, higher θ appropriately shifts emphasis toward these bottlenecks and avoids over-investment in already robust static units within the three-month operational horizon. Overall, the results illustrate a structured yet practical approach to cost modeling in reliability allocation: by leveraging the raw cost index from expert fuzzy linguistic ratings and converting them to crisp values, instead of relying on detailed financial data that are often unavailable at early design stages. This method enables designers and reliability engineers to incorporate economic constraints into early-stage prioritization without sacrificing analytical rigor.

4.5. Weight determination & reliability allocation

Zhuang *et al* [53], proposed a reliability-allocation framework that integrates improvement potential, failure severity, and complexity of implementing enhancements. Their modified criticality index prioritizes subsystems with high severity failures that can be improved through technologically feasible and lower-effort interventions. While their approach effectively links failure impact with practical feasibility, it does not explicitly address economic constraints, which are often decisive in real-world allocation decisions. To address this limitation, a practical cost index is introduced, along with a multi-dimensional allocation model that captures the urgency, feasibility, and economic viability of reliability improvements.

In the proposed framework, the reliability-improvement weight is derived from three interacting factors: severity, which reflects the criticality of failure consequences; effort, which penalizes technically demanding improvements; and cost, which represents the financial burden of implementation. This combination prioritizes improvement actions that offer high impact while remaining attainable and economically justified. Conversely, subsystems that are deeply entrenched, complex, or costly to upgrade are deprioritized unless the associated failure severity is critically high. This ensures that limited resources are directed toward improvements that provide the greatest reduction in severity per unit of effort and cost. The composite weighting for each subsystem is then computed using the formulation given by:

$$\bar{W}_i = \frac{s_i}{e_i \times c_i} \tag{28}$$

$$W_i = \frac{\bar{W}_i}{\sum_{i=1}^{N} \bar{W}_i} \tag{29}$$

where s_i, e_i, and c_i represent the normalized severity, improvement effort, and cost indices, respectively.

This formulation encodes the severity-to-cost-effort tradeoff, directing prioritization toward subsystems where reliability improvements are simultaneously impactful (high s_i), more attainable (low e_i, low c_i). This approach balances two competing objectives: maximizing subsystem reliability in proportion to failure consequence and minimizing the total improvement effort and associated cost. Consequently, it ensures that resources are directed to areas where they yield the greatest reliability benefit per unit of investment. Unlike conventional optimization models, this framework functions as a prioritization tool that integrates expert judgment, ensuring practical alignment with real-world operational and budgetary constraints.

The reliability allocation for each subsystem R_i is traditionally expressed using an exponential relation:

$$R_i = R_{\text{sys}}^{W_i} \tag{30}$$

where $R_{\text{sys}} \in (0, 1)$ is the target system reliability and W_i is the normalized weight assigned to the subsystem i . However, this formulation yields a counterintuitive outcome: larger values of W_i lead to lower allocated reliability R_i, due to the convex nature of the exponential function in the interval (0,1). Specifically, for $W_1 < W_2$, we observe $R^{W_1} > R^{W_2}$ when $R < 1$, that more critical subsystems (those with higher W_i) are assigned lower reliability targets—contrary to engineering expectations. To resolve this inconsistency, a transformed weighting scheme is applied:

$$\omega_i = \frac{1 - W_i}{\sum_{i=1}^{N} (1 - W_i)}. \tag{31}$$

This transformation ensures that subsystems with higher criticality weights, derived from failure severity or cost-effort considerations, receive correspondingly higher reliability targets. As $\omega_i \to 0$, the allocated reliability approaches unity ($R_i \to 1$), satisfying the practical design expectation that overly critical subsystems should be engineered to achieve higher reliability target. Conversely, as $\omega_i \to 1$, the allocated reliability approaches R_{sys} ($R_i \to R_{\text{sys}}$), indicating a relaxed requirement for lower-priority subsystems. This transformation aligns the mathematical model with intuitive reliability allocation principles, as discussed by [54], and [55]. Using these transformed weights, the reliability target for each equipment group, R_E^* in a series configuration is subsequently derived as:

$$R_E^* = \left[R_{\text{Target}}^*\right]^{\omega_i} \tag{32}$$

where R_{Target}^* is the overall system reliability target, set at a quarterly value of 90% to ensure required operational availability. This target underscores both the criticality of the system and the operational emphasis on maintaining high equipment uptime. Given the series–parallel configuration implemented for the evaporator system, where equipment groups function in series, equation (32) is applied to compute the required reliability of each equipment group, R_E^*. This formulation ensures that allocated reliability targets assigned to each equipment group are commensurate with their relative criticality within the system architecture.

Table 8 summarizes the transformed severity, effort, and composite cost indices used to derive the allocation weights for the equipment groups. Once system-level reliability has been

Table 8. Transformed severity, effort, and cost indices for equipment group reliability weight allocation.

i Equipment	S_i (equation (16))	$\bar{S}_i$ (equation (17))	s_i (equation (18))	E_i (equation (19))	e_i (equation (20))	$\bar{C}_i$ (equation (23))	c_i (equation (27))
1 Feed pumps	7.89	551.15	0.315 441	0.012 273	0.114 198	2.521 349	0.350 617
2 Evaporator	7.22	322.47	0.184 559	0.042 651	0.396 865	1.079 152	0.150 066
3 Recirculation pump	7.89	551.15	0.315 441	0.017 466	0.162 515	2.521 349	0.350 617
4 Heat exchanger	7.22	322.47	0.184 559	0.035 081	0.326 422	1.069 323	0.148 699

Note: In alignment with literature ([46]; [53]), a value of $r = 100$, $a = 0.8$ is adopted in this study to estimate improvement efforts and amplified severity effects.

allocated to each group, the next step is to further distribute the group reliability to individual equipment units based on the k-out-of-n configuration governing each group. Since the reliability of an equipment group is solely a function of the reliabilities of its constituent equipment, the computed group reliability value is substituted into equation (6) as:

$$R_E^* = f\left(R_{E,T}^*\right) = \sum_{k=2}^{3} \begin{pmatrix} 3 \\ 2 \end{pmatrix} {R_{E,T}^*}^K \left(1 - R_{E,T}^*\right)^{3-k}. \quad (33)$$

This equation enables the analytical derivation of individual equipment reliability, $R_{E,\,T}^*$ such that the combined reliability of all units within the group meets the overall group target. Solving equation (33) provides the specific reliability targets for each equipment operating under the defined configuration. The results of this calculation are summarized in table 9 for an evaluation period of $t = 3$ months, providing a detailed breakdown of the required reliability targets for each individual equipment within their respective groups.

Table 9 highlights that the feed and recirculation pumps represent as reliability bottleneck in the evaporation system, limiting the achievement of the target system reliability of 90% over a three-month operational interval. Conversely, static equipment such as evaporator and heat exchanger exceeds their allocated reliability targets, largely due to their predominant wear-out failure patterns, which manifest over longer periods than the quarterly assessment period. The quarterly reliability assessment aligns with the plant's preventive maintenance strategy, wherein scheduled interventions facilitate functional restoration, thereby mitigating degradation and reducing the probability of in-service failures.

4.6. Comparative allocation performance

The proposed framework discourages over-allocation to already robust static units by amplifying the economic penalty associate with pushing components toward their reliability limits, where costs escalate rapidly. Consequently, it does not seek to further raise the high reliability of static equipment within the 3 month horizon. Instead, it reallocates emphasis to rotating equipment, the feed and recirculation pumps, which exhibit lower baseline reliability dominated by seal and vibration failures and therefore offer higher marginal gains per unit effort and cost. The observation that the evaporator and heat exchanger exceed their allocated targets reflects longer wear-out modes, which extend beyond the analysis timescale. As demonstrated in section 4.4, increasing θ appropriately shifts weight toward high-C_i subsystems (the pumps) and away from static units, aligning improvements with the actual reliability bottlenecks indicated by plant data and failure modes. In doing so, the framework addresses a key gap in the research, which often overlooks the economic consequences of incremental reliability improvements and therefore fails to generate the economically rational reallocation needed when marginal reliability gains vary sharply across equipment classes.

This distinction becomes evident in the allocation outcomes, as illustrated in figure 8, which shows the practical implications of the cost-sensitive allocation. For the feed pump, the proposed model assigns a 0.913 36 target, outperforming [53], 0.866 61 and [42], 0.906 62, thereby prioritizing equipment with historically lower reliability without triggering excessive cost escalation. For the recirculation pump, the proposed target 0.905 34 likewise balances subsystem improvements, surpassing [53], 0.886 96 and slightly exceeding [42], 0.900 32. For static equipment, the proposed approach de-emphasizes near-limit targets while maintaining competitive reliability: the evaporator target (~0.897 65) is lower than [53], 0.943 68 and approximately equal to [42], (~0.897 65); the heat exchanger target (~0.899 82) is lower than both [53], 0.938 97 and [42], 0.903 80. This prevents overspend on already robust static units and shifts focused toward rotating-equipment bottlenecks where marginal gains per unit effort and cost are larger.

This behavior contrasts with [53], and [42], whose methods can over-allocate to already robust equipment because they do not explicitly model nonlinear cost escalation. By incorporating a fuzzy-based cost index and a severity–effort–cost weighting, the proposed framework achieves a more uniform and economically rational distribution of reliability, strengthening its applicability to complex industrial systems where cost–reliability trade-offs are decisive.

Beyond pumps, the proposed methodology is applicable to other industrial systems where modular design and redundancy are prevalent. Fuzzy-based reliability optimization has been demonstrated across diverse domains: compressor networks in HVAC systems, where fuzzy logic combined with machine learning improved predictive maintenance and reduced downtime [56]; multi-unit pumping configurations, where incorporating fuzzy failure and repair rates into MTBF estimates produced more accurate reliability predictions under uncertainty [57]; and food processing sector, where a neuro-fuzzy method in a flour milling plant enhanced

Table 9. Computed reliability weights and target reliability allocation for equipment groups and individual units, based on a 90% system reliability target at $t = 3$ months.

i	Equipment	$\overline{W}_i$ (equation (28))	W_i (equation (29))	ω_i (equation (31))	Equipment group reliability target, R_E^* (equation (32))	Individual equipment reliability target, $R_{E,T}^*$ (equation (33))	Actual equipment reliability, $R_{E,T}$	% Improvement required
1	Feed pumps	7.878 178	0.387 794	0.204 069	0.978 729	0.913 357	0.423 334	115.75%
2	Evaporator	3.098 921	0.152 541	0.282 486	0.970 676	0.897 651	0.999 999	$R_{E,\,T} > R_{E,\,T}^*$
3	Recirculation pump	5.535 945	0.272 501	0.242 500	0.974 774	0.905 335	0.692 874	30.66%
4	Heat exchanger	3.802 305	0.187 164	0.270 945	0.971 857	0.899 823	0.999 401	$R_{E,\,T} > R_{E,\,T}^*$

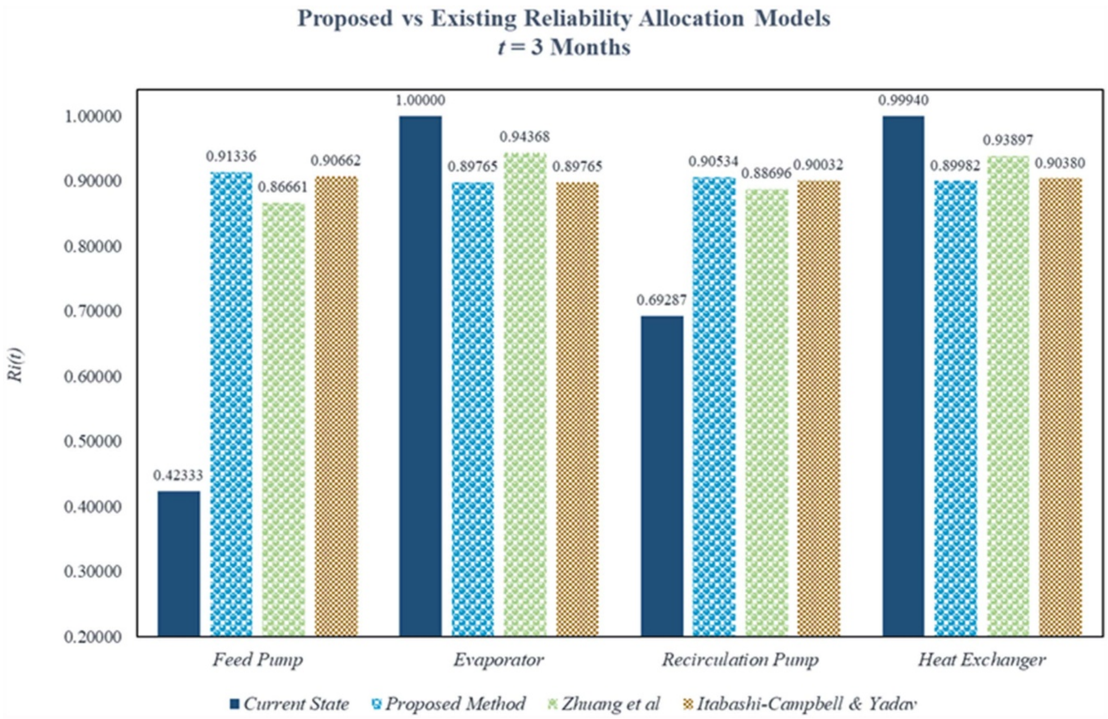

Figure 8. Comparison of actual versus computed reliability targets for individual equipment at $t = 3$ months under the proposed and existing allocation models.

failure anticipation and reduced maintenance costs [58]. These examples underscore the versatility of fuzzy-based frameworks for improving reliability in complex engineered systems with uncertain design and operational data. Knowing the reliability target for each equipment is critical not only for design improvement but also for monitoring failure rates and implementing proactive measures. With clear reliability expectations, operation and maintenance teams can track equipment performance, identify deviations promptly, and take pre-emptive measures to avoid failures.

5. Conclusion

A structured reliability allocation framework was implemented, in which system-level targets were systematically decomposed and assigned to equipment groups and, ultimately, to individual equipment. A key contribution of this work is the introduction of a transformed, dimensionless cost index, formulated using an exponential function to reflect the nonlinear escalation of design costs as systems approach practical reliability limits. Integrating this index into the multi-criteria allocation process enabled a balanced consideration of failure severity, improvement effort, and cost, yielding reliability targets that are both technically justified and economically realistic.

Given that the analysis was conducted for a multi-train evaporation system in an early design phase, detailed monetary cost data were not yet available. Under such conditions, the use of proxy cost indices and fuzzy expert elicitation is appropriate; however, broader applicability will require validation of proxy-to-cost relationships against realized project data, as well as consideration of equipment interactions that extend beyond the independence assumptions inherent in conventional RBD modeling.

Despite its methodological simplicity, the framework provides a robust basis for identifying reliability constraints and prioritizing equipment-level improvements. Incorporating insights from operations and maintenance personnel ensured that historical failure data was interpreted within their practical context, leading to more realistic allocation outcomes. Applying the method during preliminary design also allowed early identification of system vulnerabilities, facilitated proactive redundancy planning, and clearly delineated the contribution of individual equipment to both group-level and system-level reliability.

Data availability

Data supporting the findings of this study are available from the corresponding author upon reasonable request.

Conflict of interest

The author reports that there are no competing interests to declare.

Funding details

This investigation did not receive financial support from any funding entity, whether public, commercial, or not-for-profit.

Authors' contributions

The author conducted the study, analyzed the findings, and composed the manuscript.

ORCID iD

Mohammad Rahman 0009-0003-5483-1125

References

[1] Wang Z H 1992 *Reliability Engineering Theory and Practice* (Quality Control Society of the Republic of China)
[2] Oszczypała M, Konwerski J, Ziółkowski J and Małachowski J 2024 Reliability analysis and redundancy optimization of k-out-of-n systems with random variable k using continuous time Markov chain and Monte Carlo simulation *Reliab. Eng. Syst. Saf.* **242** 109780
[3] Alven W H 1964 *Reliability Engineering Prepared by ARINC Research Corporation* (Prentice Hall)
[4] Advisory Group of Reliability of Electronic Equipment (AGREE) 1957 *Reliability of Military Electronic Equipment* (Office of the Assistant Secretary of Defense Research and Engineering)
[5] Anderson R T 1976 *Reliability Design Handbook* (Defense Technical Information Center, ITT Research Institute)
[6] Boyd J 1992 Allocation of reliability requirements: a new approach *Proc. Reliability and Maintainability Symp.* (*Las Vegas, Nevada, USA*) pp 5–6
[7] Di Bona G, Forcina A and Silvestri A 2016 Critical flow method: a new reliability allocation approach for a thermonuclear system *Qual. Reliab. Eng. Int.* **32** 1677–91
[8] Di Bona G and Forcina A 2017 Analytic critical flow method: a reliability allocation method based on analytic hierarchy process *J. Fail. Anal. Prev.* **17** 1149–63
[9] Di Bona G, Falcone D, Silvestri A and Forcina A 2018 IFM target 2.0: an innovative method to define reliability target for prototype systems *Int. J. Adv. Manuf. Technol.* **95** 3349–67
[10] Felice F D, Bona G D, Falcone D and Silvestri A 2010 New reliability allocation methodology: the integrated factors method *Int. J. Oper. Quant. Manage.* **16** 67–85
[11] Di Bona G, Forcina A, Petrillo A, De Felice F, Silvestri A and Madu C 2016 A-IFM reliability allocation model based on multicriteria approach *Int. J. Qual. Reliab. Manage.* **33** 676–98
[12] Di Bona G, Silvestri A, Forcina A and Falcone D 2017 AHP-IFM target: an innovative method to define reliability target in an aerospace prototype based on analytic hierarchy process *Qual. Reliab. Eng. Int.* **33** 1731–51
[13] Chang Y-C, Chang K-H and Liaw C-S 2009 Innovative reliability allocation using the maximal entropy ordered weighted averaging method *Comput. Ind. Eng.* **57** 1274–81
[14] Kim K O, Yang Y and Zuo M J 2013 A new reliability weight for reducing the occurrence of severe failure effects *Reliab. Eng. Syst. Saf.* **117** 81–88
[15] Kim K O and Zuo M J 2018 General model for the risk priority number in failure mode and effects analysis *Reliab. Eng. Syst. Saf.* **169** 321–9
[16] Wang Y, Yam R C M, Zuo M J and Tse P 2001 A comprehensive reliability allocation method for design of CNC lathes *Reliab. Eng. Syst. Saf.* **72** 247–52
[17] Yousefi S, Alizadeh A, Hayati J and Baghery M 2018 HSE risk prioritization using robust DEA-FMEA approach with undesirable outputs *Saf. Sci.* **102** 144–58
[18] Chen Z, Liu Y, Huang H, Wu X and He L 2013 A reliability allocation method considering failure dependence *Proc. ASME 2013 IDETC/CIE* p V008T12A006
[19] Yi X, Dhillon B S, Shi J, Mu H and Hou P 2017 Reliability optimization allocation method for multifunction systems with multistate units based on goal-oriented methodology *ASME J. Risk Uncertain. B* **3** 041010
[20] Du Y, Lu X, Su X, Hu Y and Deng Y 2016 New failure mode and effects analysis: an evidential downscaling method *Qual. Reliab. Eng. Int.* **32** 737–46
[21] Liu H-C, Liu L and Liu N 2013 Risk evaluation approaches in failure mode and effects analysis: a literature review *Expert Syst. Appl.* **40** 828–38
[22] Lo H-W and Liou J J H 2018 A novel multiple-criteria decision-making-based FMEA model for risk assessment *Appl. Soft Comput.* **73** 684–96
[23] Mohammadi M, Mortazavi S and Karbasian M 2018 Developing a method for reliability allocation of series-parallel systems by considering common cause failure *Int. J. Ind. Eng. Prod. Res.* **29** 213–30
[24] Elegbede A O, Chu C, Adjallah K H and Yalaoui F 2003 Reliability allocation through cost minimization *IEEE Trans. Reliab.* **52** 106–11
[25] Majety S R V, Dawande M and Rajgopal J 1999 Optimal reliability allocation with discrete cost-reliability data for components *Oper. Res.* **47** 899–906
[26] Cruz J 2016 Applicability and limitations of reliability allocation methods NASA/TM-2016-218488
[27] Mettas A 2000 Reliability allocation and optimization for complex systems *Proc. Annual Reliability and Maintainability Symp. (RAMS)*
[28] Hammood H K and Al-Khafaji Z 2025 Harmony search algorithm for optimal reliability allocation with cost-reliability data for components *AIP Conf. Proc.* **3264** 050011
[29] Punia P, Raj A and Kumar P 2024 Enhanced zebra optimization algorithm for reliability redundancy allocation and engineering optimization problems *Cluster Comput.* **28** 267
[30] Chowdury M A M, Nath R, Shukla A K, Rauniyar A and Muhuri P K 2024 Multi-task optimization in reliability redundancy allocation problem: a multifactorial evolutionary-based approach *Reliab. Eng. Syst. Saf.* **244** 109807
[31] Guan B, Li Z, Coit D W and Li Y-F 2024 Review of the redundancy allocation problem to optimize system reliability *Eng. Optim.* **57** 44–68
[32] Mahato S K, Bhattacharyee N and Pramanik R 2020 Fuzzy reliability redundancy optimisation with signed distance method for defuzzification using genetic algorithm *Int. J. Oper. Res.* **37** 307–23
[33] Paramanik R, Mahato S K, Bhattacharyee N, Supakar P and Sarkar B 2020 Multiple constrained reliability-redundancy optimization under triangular intuitionistic fuzziness using a genetic algorithm *Reliability Management and Engineering* (CRC Press) pp 205–32
[34] Bhattacharyee N, Paramanik R and Mahato S K 2020 Optimal redundancy allocation for the problem with chance constraints in fuzzy and intuitionistic fuzzy environments

using soft computing technique *Ann. Optim. Theory Pract.* **3** 25–47
[35] Paramanik R, Kumar N and Mahato S K 2022 Solution for the optimality of an intuitionistic fuzzy redundancy allocation problem for complex system using Yager's ranking method of defuzzification with soft computation *Int. J. Syst. Assur. Eng. Manage.* **13** 615–24
[36] Misra K B 1992 *Reliability Analysis and Prediction: A Methodology-oriented Treatment* (Elsevier)
[37] Abernethy R B 2000 *The New Weibull Handbook* 5th edn (Robert B. Abernethy)
[38] ReliaSoft 2007 *Reliability Engineering Resource Handbook* (ReliaSoft Corporation)
[39] Barlow R E and Proschan F 1965 *Mathematical Theory of Reliability* (Wiley)
[40] Sun Y 2006 Reliability prediction of complex repairable system: an engineering approach
[41] Yadav O P, Singh N and Goel P S 2006 Reliability demonstration test planning: a three-dimensional consideration *Reliab. Eng. Syst. Saf.* **91** 882–93
[42] Itabashi-Campbell R and Yadav O 2009 *System Reliability Allocation based on FMEA Criticality* (SAE Technical Paper) (https://doi.org/10.4271/2009-01-0202)
[43] Xiao N, Huang H-Z, Li Y, He L and Jin T 2011 Multiple failure modes analysis and weighted risk priority number evaluation in FMEA *Eng. Fail. Anal.* **18** 1162–70
[44] Gu Y and Tang S 2010 A fuzzy reliability allocation method for the product based on the knowledge *Proc. 2010 Int. Conf. Measuring Technology and Mechatronics Automation* pp 101–4
[45] Sriramdas V, Chaturvedi S K and Gargama H 2014 Fuzzy arithmetic based reliability allocation approach during early design and development *Expert Syst. Appl.* **41** 3444–9
[46] Cheng Q, Kang Y, Yang C, Zhang C and Chen C 2023 A new reliability allocation method for machine tools based on ITrFNs and AHP-GRA *Int. J. Adv. Manuf. Technol.* **124** 4019–32
[47] Liang Q 2022 Reliability allocation of sonar based on fuzzy hierarchy method *Proc. 2022 IEEE Int. Conf. Sensing, Diagnostics, Prognostics, and Control (SDPC)* pp 166–9
[48] Yadav O P and Zhuang X 2014 A practical reliability allocation method considering modified criticality factors *Reliab. Eng. Syst. Saf.* **129** 57–65
[49] Yu H, Zhang G, Ran Y, Li M and Wang Y 2018 A comprehensive and practical reliability allocation method considering failure effects and reliability costs *Eksploatacja i Niezawodnosc—Maint. Reliab.* **20** 244–51
[50] Aggarwal K 1993 *Reliability Engineering* ed Z Kellers (Springer) (https://doi.org/10.1007/978-94-011-1928-3)
[51] Kuo W, Prasad V R, Tillman F A and Hwang C L 2001 *Optimal Reliability Design* (Cambridge University Press)
[52] Falcone D, Felice F D, Di Bona G and Silvestri A 2004 R.A.M.S. analysis in a sintering plant by the employment of a new reliability allocation method *15th Int. Conf. on Modeling and Simulation* (*Marina del Rey, USA*) pp 383–8
[53] Zhuang X, Limon S M and Yadav O P 2014 Considering modified criticality factor and functional dependency for reliability allocation purposes *Proc. of the 2014 Industrial and Systems Engineering Research Conf.* (*Montreal, Canada*)
[54] Dhillon B S 2006 *Maintainability, Maintenance, and Reliability for Engineers* (CRC Press)
[55] Zio E 2007 *An Introduction to the Basics of Reliability and Risk Analysis* (World Scientific) (https://doi.org/10.1142/6442)
[56] Bisal P and Jana P 2025 Compressor health monitoring and predictive maintenance by anomaly detection using fuzzy logic and random forest model *Int. J. Mach. Tools Maint. Eng.* **6** 1–6 (available at: www.mechanicaljournals.com/ijmtme/article/48/5-2-13-707.pdf)
[57] Mortazavi S M, Mohamadi M and Jouzdani J 2018 MTBF evaluation for 2-out-of-3 redundant repairable systems with common cause and cascade failures considering fuzzy rates for failures and repair *J. Ind. Eng. Int.* **14** 281–91
[58] Brisco N D A 2025 Optimization of equipment reliability based on a neuro-fuzzy approach: case of a flour mill *Reliability: Theory & Applications* pp 865–82

Mohammad Rahman serves as a Global Reliability Engineer at Rio Tinto Group, USA. He specializes in industrial system reliability, probabilistic risk assessment, and maintenance optimization. His work focuses on applying data-driven decision-support methods to enhance the availability and performance of complex process systems. He has led numerous reliability initiatives across the chemical, power, and nuclear industries, with emphasis on failure-mode analysis, reliability-centered maintenance (RCM), and asset-management strategies. His research interests include redundancy optimization, decision modeling, and the integration of condition-monitoring technologies into physical asset-management frameworks.